

Some theoretical results concerning O₃-NO_x-VOC chemistry and NO_x-VOC indicators

Sanford Sillman and Dongyang He

Department of Atmospheric, Oceanic and Space Sciences, University of Michigan, Ann Arbor, Michigan, USA

Received 18 July 2001; revised 7 June 2002; accepted 7 June 2002; published 29 November 2002.

[1] A series of model results is shown pertaining to ozone, reactive nitrogen (NO_y), and peroxides in polluted regions. The results focus on ratios such as O₃/NO_y and H₂O₂/HNO₃ that have been proposed as indicators for O₃-NO_x-VOC sensitivity. These ratios are shown to correlate with predicted NO_x-VOC sensitivity for a variety of zero-dimensional (0-D) and 3-D models, but the correlation varies in situations ranging from relatively clean to highly polluted. The previously identified NO_x-VOC transition values for indicators appear to be valid for moderately polluted conditions with 80–150 ppb O₃. Changes in indicator behavior are linked to odd hydrogen chemistry and in particular to changes in the ratio of O₃ to primary radical production. Changes in indicator behavior are also correlated with the values of a test ratio, O₃/(2H₂O₂+NO_z) which can be evaluated against measurements. Ratios of the form ΔO₃/ΔNO_y, representing differences relative to background values, are proposed for analyzing NO_x-VOC sensitivity in individual urban plumes. Comparisons are made to extent-of-reaction parameters, which have been proposed for evaluating NO_x-VOC sensitivity. *INDEX TERMS*: 0365 Atmospheric Composition and Structure: Troposphere—composition and chemistry; 0345 Atmospheric Composition and Structure: Pollution—urban and regional (0305); 3210 Mathematical Geophysics: Modeling; *KEYWORDS*: ozone, nitrogen oxides, volatile organic compounds (VOC), hydrogen peroxide, photochemical smog

Citation: Sillman, S., and D. He, Some theoretical results concerning O₃-NO_x-VOC chemistry and NO_x-VOC indicators, *J. Geophys. Res.*, 107(D22), 4659, doi:10.1029/2001JD001123, 2002.

1. Introduction

[2] The chemistry of ozone and its two main precursors, NO_x and volatile organic compounds (VOC), continues to represent one of the major uncertainties in the field of atmospheric chemistry. In urban areas, uncertainty associated with O₃-NO_x-VOC chemistry can affect the design of control strategies to reduce ambient O₃. In the remote troposphere, O₃-NO_x-VOC chemistry affects evaluations of the ozone production efficiency per NO_x as well as predicted responses to future changes in emissions.

[3] In recent years a number of works have analyzed the photochemical factors that determine the split into VOC-sensitive and NO_x-sensitive regimes [Sillman *et al.*, 1990; Sillman, 1995; Kleinman, 1994; Kleinman *et al.*, 1997; Tonnesen and Dennis, 2000a, 2000b; Jaegle *et al.*, 1998, 2001]. Sillman [1995] and Sillman *et al.* [1998] proposed that O₃-NO_x-VOC chemistry could be linked to the ratios of certain measurable species which had different values for NO_x-sensitive and VOC-sensitive conditions. If successful, these “NO_x-VOC indicators” can provide a powerful tool for evaluating the chemical process leading to ozone formation. However, there is a range of theoretical and practical concerns associated with the proposed indicators. Contradictory results were reported by Lu and

Chang [1998] and Chock *et al.* [1999]. It is especially unclear whether the indicator ratios would show similar behavior for a wide variety of conditions, as proposed by Sillman.

[4] Here, a series of model calculations is used to explore indicator behavior for a variety of conditions, ranging from rural to extremely polluted conditions. The calculations have two purposes: to identify how the behavior of indicator ratios may vary under different conditions; and to identify the link between the proposed indicator ratios and the chemistry of odd hydrogen radicals. The link between indicator ratios and odd hydrogen radicals, presented previously by Sillman [1995], Kleinman [1994], and Kleinman *et al.* [1997] will be used to explain variations in the behavior of indicator ratios for different conditions. Model results will also be used to identify broad correlation patterns among ozone, reactive nitrogen, and peroxides that are associated with NO_x-sensitive and VOC-sensitive chemistry.

[5] Results will be shown from both zero-dimensional (0-D) calculations and 3-D models. It should be emphasized that valid predictions for species concentrations must be based on 3-D models, which include more detailed representation of dynamical processes and which include comparison with measured values. The 0-D calculations are useful because they can extend previous analyses to new conditions (which do not match observed cases, but which may correspond to future situations) and because they allow

a more detailed analysis of the chemical factors which drive the results.

2. Theoretical Background

[6] The split between NO_x-sensitive and VOC-sensitive conditions is well-known, and illustrated by ozone isopleth plots (e.g., see Figure 1). For conditions with relatively high VOC and low NO_x, O₃ increases with increasing NO_x and is relatively insensitive to changes in VOC. For conditions with relatively low VOC and high NO_x, O₃ increases with increasing VOC and decreases with increasing NO_x. An analogous split between “NO_x-sensitive” and “NO_x-saturated” regimes occurs in the remote troposphere, although for remote conditions O₃ increases with increasing VOC even in the NO_x-sensitive regime [Jaegle *et al.*, 1998, 2001].

[7] The split between NO_x-sensitive and VOC-sensitive regimes is driven by the chemistry of odd hydrogen radicals. As shown by Sillman *et al.* [1990] and Sillman [1995], the NO_x-VOC split was attributed to the relative rate of formation of peroxides (via HO₂-HO₂ and HO₂-RO₂ reactions) relative to nitric acid formation (via OH + NO₂). NO_x-sensitive conditions occur when peroxides dominate over nitric acid as radical sinks, while NO_x-saturated conditions occur when nitric acid dominates. As shown by Kleinman [1994], NO_x-VOC sensitivity was attributed to the relative source strengths of odd hydrogen radicals (S_H) and odd nitrogen (S_N), summed over the period of ozone production for an air parcel. (Abbreviations are summarized in section 8.) VOC-sensitive chemistry occurred when the odd nitrogen source exceeded the source of odd hydrogen. Subsequently Kleinman *et al.* [1997] found that the instantaneous rate of ozone production was VOC-sensitive whenever the instantaneous loss rate for odd nitrogen (L_N) was greater than half the total odd hydrogen source (L_N/Q > 0.5, as given by Kleinman *et al.* [1997]). This formulation is equivalent to that of Sillman [1995] if net formation of PAN and other organic nitrates is assumed to be zero. From Sillman [1995], odd hydrogen sources must be in steady state with its three major sinks:

$$S_H = 2P_{\text{perox}} + P_{\text{HNO}_3} + P_{\text{pans}} \quad (1)$$

where P_{perox} and P_{HNO₃} represent production rates for peroxides (including H₂O₂ and organic peroxides) and HNO₃, and P_{pans} represents net photochemical production of PAN and higher order analogues. VOC-sensitive chemistry would occur whenever P_{HNO₃} exceeds 2P_{perox}. In terms of S_H, VOC-sensitive chemistry would occur for the following conditions:

$$S_H < \xi L_N \quad (2a)$$

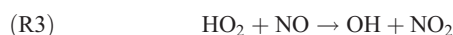
$$\xi = 1 + \frac{P_{\text{HNO}_3}}{P_{\text{HNO}_3} + P_{\text{PANs}}} \quad (2b)$$

or

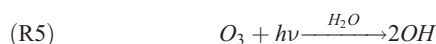
$$S_H - P_{\text{pans}} < 2P_{\text{HNO}_3} \quad (2c)$$

[8] This modified form serves to emphasize that the NO_x-VOC split is associated with formation of nitric acid but is not affected by formation of PAN [Sillman *et al.*, 1990; Tonnesen and Dennis, 2000b].

[9] The above results were derived by Sillman [1995] and Kleinman *et al.* [1997] based on the following simplified photochemistry. The ozone production sequence includes



[10] Similar reaction sequences apply for many individual VOC, which produce various radical chains with the form RO₂ and with subsequent reactions analogous to (R2). Reaction (R1) (VOC + OH) is the rate limiting step for this sequence, and its rate depends on the availability of OH. OH in turn depends on the balance of sources and sinks of odd hydrogen radicals (including OH, HO₂ and RO₂), which includes the following sources

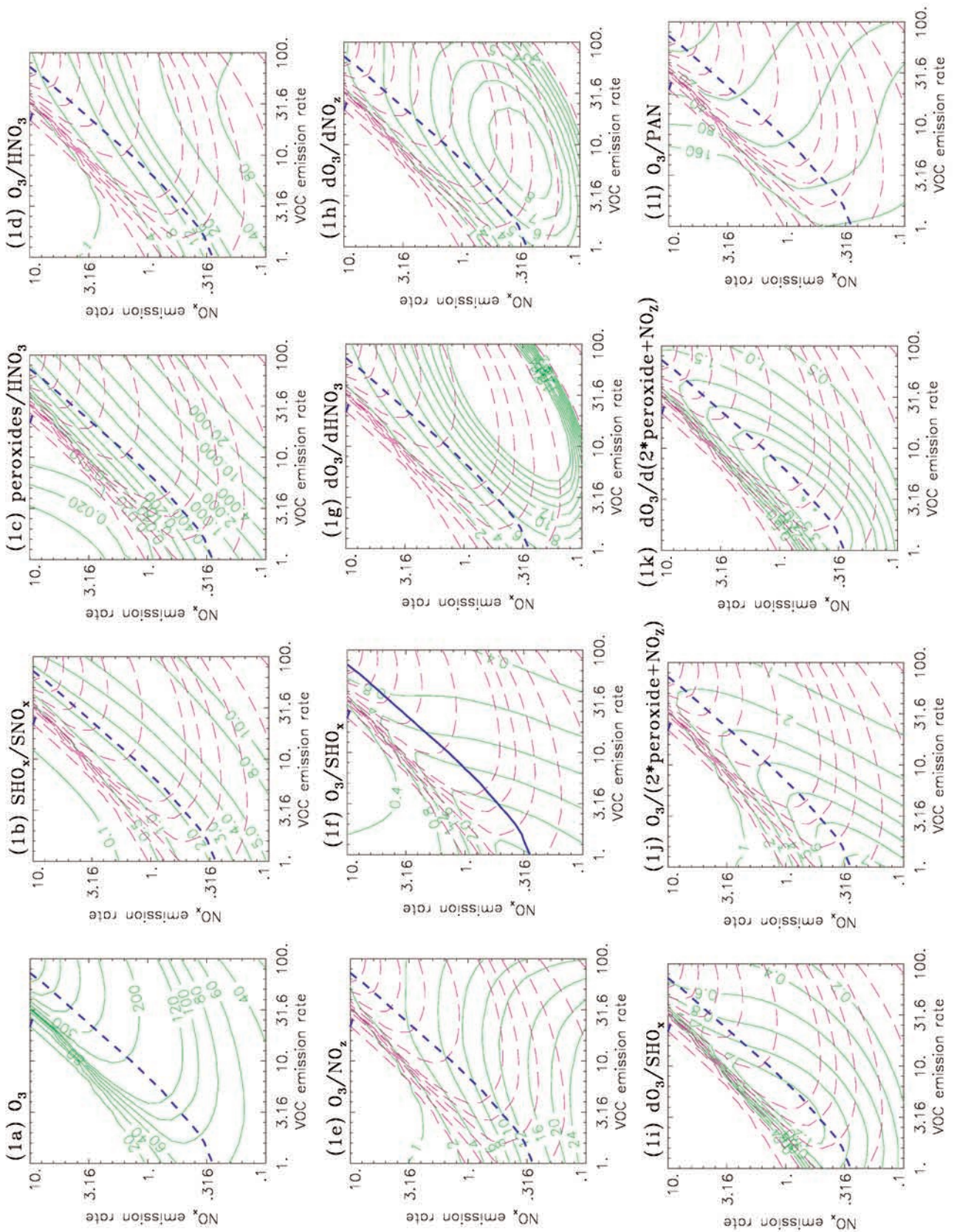


[11] Other sources include the photolysis of higher aldehydes and various alkene-O₃ reactions [Paulson and Orlando, 1996]. Sinks include the following.



where (R10) refers to net production of PAN. As first developed by Sillman *et al.* [1990], when the peroxide-

Figure 1. (opposite) Isopleths as a function of the average emission rate for NO_x and VOC (10¹² molec. cm⁻² s⁻¹) in 0-D calculations. The isopleths represent conditions in the first layer during the afternoon following 3-day calculations, at the hour corresponding to maximum O₃. Isopleths are shown for (a) O₃ (ppb); (b) S_H/S_N; (c) (H₂O₂ + ROOH)/HNO₃; (d) O₃/HNO₃; (e) O₃/NO_z; (f) O₃/S_H; (g) ΔO₃/ΔHNO₃; (h) ΔO₃/ΔNO_z; (i) ΔO₃/S_H; (j) O₃/(2H₂O₂ + 2ROOH + NO_z); (k) ΔO₃/Δ(2H₂O₂ + 2ROOH + NO_z); and (l) O₃/PAN. Isopleths are shown as solid green lines. Isopleths for O₃ (red dashed lines) are superimposed on the other isopleth plots. The short blue dashed line represents the transition from VOC-sensitive to NO_x-sensitive conditions.



forming reactions (R7) and (R8) are the dominant radical sinks, then the radical steady state reduces to

$$HO_2 \propto \sqrt{S_H - P_{pans}} \quad (3)$$

where the similar but more complex RO₂ has been omitted for simplicity. The production rate for O₃ is approximately equal to the rate of reactions (R2) and (R3) (HO₂ + NO, RO₂ + NO). This rate increases with increasing NO_x but has little direct dependence on VOC. By contrast, when the reaction to form nitric acid (R9) is the dominant radical sink, then the radical steady state becomes

$$OH \propto (S_H - P_{pans})/NO_2 \quad (4)$$

[12] The production rate for O₃ is proportional to the rate of the VOC + OH reactions (R1), and this rate increases with increasing VOC and decreases with increasing NO_x.

[13] *Tonnesen and Dennis* [2000a] presented a similar results with slightly different terminology. Tonnesen and Dennis analyzed ozone formation in terms of radical formation (equivalent to S_H here), radical termination (through production of peroxides, HNO₃ and organic nitrates) and radical propagation (through VOC + OH and HO₂ + NO, reactions (R1), (R2), and (R3)). The radical propagation reactions are directly associated with ozone formation and were regarded as synonymous with ozone production in *Sillman* [1995].

[14] *Kleinman et al.* [1997], *Tonnesen and Dennis* [2000a], and *Kirchner et al.* [2001] have developed methods for evaluating whether the instantaneous rate of ozone production is sensitive to NO_x or VOC. This instantaneous sensitivity should be distinguished from the sensitivity associated with ozone concentrations, which are affected by upwind emissions, transport, and photochemistry. As discussed by *Kirchner et al.* [2001], *Sillman* [1995] identified indicator ratios that relate specifically to the NO_x-VOC sensitivity of ozone concentrations rather than instantaneous production rates. The subsequent results all relate to the NO_x-VOC dependence of ozone concentrations, based on photochemical production over extended periods of time.

[15] The NO_x-VOC indicators proposed by *Sillman* [1995] included the following: O₃/NO_y (where NO_y represents total reactive nitrogen); O₃/NO_z (where NO_z represents summed NO_x reaction products, or NO_y-NO_x); O₃/HNO₃; H₂O₂/HNO₃; H₂O₂/NO_z; and the equivalent ratios with summed H₂O₂ and organic peroxides. The ratios involving peroxides were justified based on the role of peroxides and nitric acid as sinks for odd hydrogen radicals. It is more difficult to explain why ratios such as O₃/NO_z should be associated with NO_x-VOC sensitivity. *Sillman* [1995] suggested that O₃ was roughly proportional to the odd hydrogen source, S_H. The ratio O₃/NO_z is then analogous to S_H/L_N, which is related to NO_x-VOC sensitivity for reasons given above. This will be discussed in more detail in section 4.

3. Methods

[16] Results will be shown from a series of simplified 0-D calculations and from previously published 3-D

model simulations. The 0-D calculations use 2-layer model [*Sillman et al.*, 1990] which has been adapted from urban photochemical box models. The model consists of a lower layer, representing the ambient boundary layer, and an upper residual layer representing conditions aloft at night. During the morning hours the height of the lower layer expands and the contents of the residual layer become entrained into the model lower layer. During the evening hours the height of the lower layer decreases and the remainder becomes part of the residual layer. The height of the lower layer varies from 200 m. at night to 1500 m. in the afternoon, representing typical behavior for a boundary layer during pollution events. The model residual layer extends from the top of the lower layer up to 1600 m. Emissions are entered into the lower layer as concentrations based on specified emission rates and the layer height. Although this model includes some rudimentary dynamics in one (vertical) dimension, it will be referred to as a 0-D model, as realistic dynamics are not included.

[17] Photochemistry and dry deposition are as shown by *Sillman et al.* [1998]. The photochemical mechanism is based on the work of *Lurmann et al.* [1986] with various modifications, including updated reaction rates from *DeMore et al.* [1997], isoprene chemistry from *Paulson and Seinfeld* [1992], RO₂-RO₂ reactions from *Kirchner and Stockwell* [1996], and organic peroxide reaction rates from *Stockwell et al.* [1997]. Aerosol reactions are not included. One weakness of this photochemical representation is that it has not been tested against environmental chamber experiments. By contrast, the RACM [*Stockwell et al.*, 1997] and SAPRC [*Carter*, 2000] have been extensively tested against chamber data. The current mechanism has been retained here because it includes many reactions that are important in the rural/remote troposphere. Also, because aerosol reactions are not included, the calculations do not account for the formation of aerosol nitrate (NO₃⁻) from heterogeneous reaction with ammonia. HNO₃ in these calculations should be viewed as equivalent to the sum of HNO₃ and NO₃⁻ [*Martilli et al.*, 2002].

[18] Calculations were performed for 3-day time periods with diurnally varying emissions, for a wide variety of anthropogenic VOC and NO_x emission rates. Speciation of VOC was based on average speciation in the NAPAP 1990 inventory [*Environmental Protection Agency (EPA)*, 1993]. Diurnal variations were based on average diurnal variations in the same inventory. In the standard series of calculations emission rates were constant (except for the diurnal variation) throughout the 3-day period. Alternative calculations were performed with higher emissions on the third day, representing a situation in which processed rural air would enter an urban area on the third day. Initial conditions were typical for remote air in the U.S.: 40 ppb O₃, 1 ppb H₂O₂, 15 ppt NO and NO₂, and 5 ppb C VOC.

[19] The 3-D simulations are summarized in Table 1.

4. Results From 0-D Calculations

[20] Figure 1 shows isopleths for O₃ and for a series of species ratios, shown as a function of diurnal average emission rates for VOC and NO_x. The plots represent

Table 1. 3-D Simulations Used in This Study^a

Location	Model	Photochemistry	Model Domain	Comparison With Measurements	Reference
Nashville*	<i>Sillman et al.</i> [1998]	modified [<i>Lurmann et al.</i> , 1986]	5 × 5 km urban; upwind domains includes eastern U.S.	O ₃ , NO _y , peroxides	<i>Sillman et al.</i> [1998]
Lake Michigan*	<i>Sillman et al.</i> [1993]	modified [<i>Lurmann et al.</i> , 1986]	20 × 20 km in region; upwind domains includes eastern U.S.	O ₃	<i>Sillman</i> [1995]
Northeast corridor*	<i>Sillman et al.</i> [1993]	modified [<i>Lurmann et al.</i> , 1986]	20 × 20 km in region; upwind domains includes eastern U.S.	O ₃	<i>Sillman</i> [1995]
Atlanta	UAM-IV [<i>Morris and Myers</i> , 1990]	CB4 [<i>Gery et al.</i> , 1989]	5 × 5 km urban	O ₃ , NO _y , isoprene, HCHO, other VOC	<i>Sillman et al.</i> [1997]
San Joaquin*	MAQSIP [<i>Odman and Ingram</i> , 1996]	CB4 [<i>Gery et al.</i> , 1989]	12 × 12 km; domain includes all central California	O ₃	<i>Sillman et al.</i> [2001]
San Joaquin	SAQM [<i>J. Chang et al.</i> , 1997]	CB4 [<i>Gery et al.</i> , 1989]	12 × 12 km; domain includes all central California	O ₃	<i>Lu and Chang</i> [1998]
Los Angeles*	UAM-IV [<i>Morris and Myers</i> , 1990]	CB4 [<i>Gery et al.</i> , 1989]	5 × 5 km urban	O ₃ , NO _y , NO ₂	<i>Godowitch and Vukovich</i> [1994]; <i>Sillman et al.</i> [1997]
Los Angeles	UAM-IV [<i>Morris and Myers</i> , 1990]	CB4 [<i>Gery et al.</i> , 1989]	5 × 5 km urban	O ₃	<i>Chock et al.</i> [1999]

^a Asterisks (*) denote models included in Figures 3–6.

conditions during the afternoon of the third day of a 3-day calculation, at the hour corresponding to maximum O₃. Figure 1a is the standard isopleth plot for O₃ and illustrates the well-known split between NO_x-sensitive and VOC-sensitive (or NO_x-saturated) conditions. Figure 1a also shows the “sensitivity transition” from NO_x-sensitive to VOC-sensitive conditions, defined as follows:

$$\frac{1}{Q_N} \frac{\partial[O_3]}{\partial Q_N} = \frac{1}{Q_H} \frac{\partial[O_3]}{\partial Q_H} \quad (5)$$

where [O₃] represents ozone concentrations and Q_N and Q_H represent emission rates for NO_x and VOC. Using this definition, the sensitivity transition represents the point at which a given percent reduction in either NO_x or VOC would result in the same reduction in O₃. As shown in Figure 1a, reduced NO_x would result in lower O₃ than an equivalent percent reduction in VOC when Q_H/Q_N is higher than its value at the transition line. When Q_H/Q_N is lower than the transition value, then reduced VOC would result in lower O₃ than an equivalent percent reduction in NO_x. The same transition line is included for reference in the other isopleth plots.

[21] Figure 1b shows the calculated ratio S_H/S_N, where S_H and S_N represent calculated sums of the source of odd hydrogen and odd nitrogen over the 3-day period. This ratio is similar to the ratio used by *Kleinman et al.* [1997] to analyze instantaneous ozone chemistry, but here they represent sums for an extended period of ozone production (including nighttime) rather than an instantaneous conditions. There is some ambiguity about this ratio in multiday calculations, because the exact value of S_H/S_N depend on the time period over which S_H is summed and because for realistic conditions an air parcel will include a wide variety of ozone production rates over its photochemical history. In

these simplified calculations, ozone production occurs continuously over the 3-day period with relatively little variation for each individual calculation. We have summed S_H and S_N over the full 3 days for both model layers as molecules produced or emitted (rather than molecules per volume). As shown below, this provides a useful way to identify differences between calculations that represent equivalent air mass histories but with very different amounts of precursors.

[22] As shown in the figure, the ratio S_H/S_N is closely associated with NO_x-VOC sensitivity and the transition from NO_x-sensitive to VOC-sensitive conditions is associated with a specific value of S_H/S_N. This transition value (S_H/S_N = 2) remains for emission rates varying by a factor of 100, and for O₃ varying from 60 to 600 ppb. Higher S_H/S_N is associated with NO_x-sensitive conditions and lower values with VOC-sensitive conditions. An equivalent transition value (L_N/S_H = 0.5) was found by *Kleinman et al.* [1997] for the NO_x-VOC variation of instantaneous ozone production. The ratio S_H/S_N cannot be measured, but it provides a theoretical basis for identifying measurable species ratios as potential NO_x-VOC indicators.

[23] The region with S_H/S_N < 1 is also of interest, because this corresponds to conditions in which the source of radicals is not sufficient to oxidize the total amount of NO_x emitted into the air mass. In this region ozone concentrations are sharply lower. The ratio NO_x/NO₃, a measure of the extent of photochemical processing, increases sharply for S_H/S_N less than one (see Figure 7). This is discussed more in section 6.

[24] Figure 1c shows the ratio (H₂O₂ + ROOH)/HNO₃. The value of this ratio is also closely associated with NO_x-VOC sensitivity, although the NO_x-VOC transition value is not uniformly constant. The transition value is 0.5 for O₃ below 250 ppb. A slightly higher value (0.5–0.6) was found in the 3-D model reported by *Sillman et al.* [1998].

At higher emission rates and higher O₃ the transition value drifts lower, reaching 0.2 at 500 ppb O₃. The NO_x-sensitive and VOC-sensitive regions of the isopleth plot are associated respectively with much higher and lower values of the ratio.

[25] The ratio H₂O₂/HNO₃ shows a similar close association with NO_x-VOC sensitivity, and again the NO_x-VOC transition value tends to decrease at higher O₃ and higher emission rates. Referring to Figure 1c, the most useful information about these ratios is the value along the sensitivity transition of the isopleth plot. These values are shown plotted against O₃ along the sensitivity transition in Figure 2. The transition value for H₂O₂/HNO₃ varies from 0.3 at 100 ppb O₃ to 0.07 at 400 ppb O₃. The transition values at 150 ppb O₃ in these calculations all correspond closely with transition values in 3-D simulations reported by *Sillman et al.* [1998].

[26] The ratio O₃/HNO₃ (Figure 1d) both show a general correspondence with NO_x-VOC sensitivity, but the correspondence is not as clear and the transition value shows greater variation. The ratio O₃/NO_z (Figure 1e) shows a significantly worse correspondence with NO_x-VOC sensitivity. There is a general (though imperfect) correspondence between O₃/NO_z and NO_x-VOC sensitivity for O₃ below 200 ppb, but the correspondence breaks down for higher O₃. When VOC emissions are high (corresponding to high O₃ at the sensitivity transition) the ratio O₃/NO_z appears to vary in direct proportion to VOC emissions and does not increase (or may even decrease) with increasing NO_x. The transition value of O₃/HNO₃ and O₃/NO_z (i.e., the value along the NO_x-VOC sensitivity transition) decreases as emission rates increase. This variation along the transition value is also shown in Figure 2b. Similar results were reported by *Tonnesen and Dennis* [2000b] and *Kirchner et al.* [2001].

[27] The behavior of O₃/NO_z and O₃/HNO₃ can be understood by regarding them as an imperfect surrogate for Kleinman's ratios S_H/S_N or S_H/L_N. It was shown above that S_H/S_N is correlated with NO_x-VOC sensitivity for the entire range of 0-D calculations used here. O₃/NO_z can be expressed as a function of S_H/L_N as follows:

$$\frac{O_3}{NO_z} = \left[\frac{S_H}{L_N} \right] \left[\frac{L_N}{NO_z} \right] \left[\frac{O_3}{S_H} \right] \quad (6a)$$

[28] Based on Figure 1b, if O₃/NO_z were directly proportional to S_H/S_N it would be expected to correlate with NO_x-VOC sensitivity and show a near-constant value along the sensitivity transition throughout the range of model calculations. To the extent that O₃/NO_z shows a different pattern, the differences should be associated with the terms L_N/NO_z and O₃/S_H in equation (6a). Therefore, L_N/NO_z and O₃/S_H may be regarded as sources of error for O₃/NO_z as a NO_x-VOC indicator.

[29] The ratio L_N/NO_z relates the rate of removal of NO_x (primarily through conversion to the species included in NO_z) to the NO_z concentration. As a source of error, this relates to the removal rate of NO_z. The ratio O₃/S_H is more important as a source of error in the indicator concept. *Sillman* [1995] assumed that S_H was likely to be proportional to O₃ because O₃ is a major precursor of odd hydro-

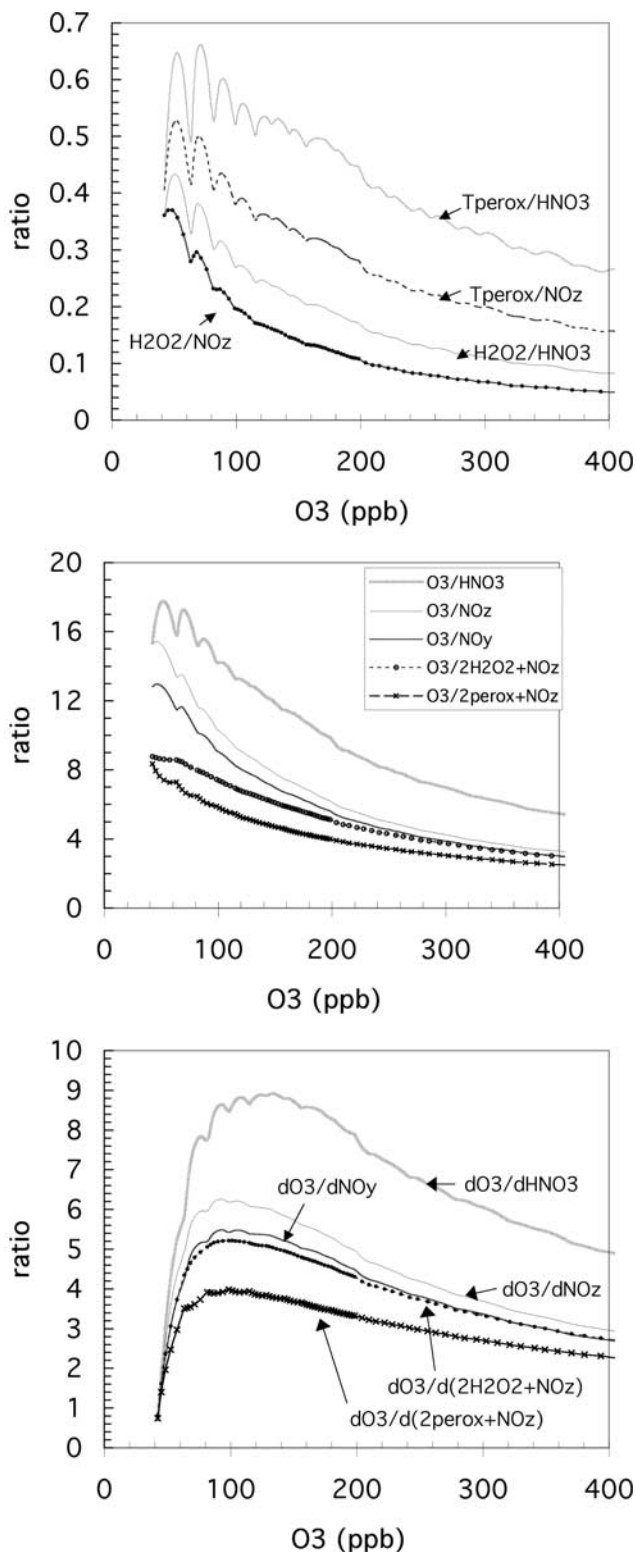


Figure 2. Values of ratios along the NO_x-VOC transition line shown in Figure 1, for 0-D calculations. Values are shown for (a) (H₂O₂ + ROOH)/HNO₃, (H₂O₂ + ROOH)/NO_z, H₂O₂/HNO₃, and H₂O₂/NO_z; (b) O₃/HNO₃, O₃/NO_z, O₃/NO_y, O₃/(2H₂O₂ + NO_z), and O₃/(2H₂O₂ + 2ROOH + NO_z) (listed in order from highest to lowest); and (c) ΔO₃/ΔHNO₃, ΔO₃/ΔNO_z, ΔO₃/ΔNO_y, ΔO₃/Δ(2H₂O₂ + NO_z), and ΔO₃/Δ(2H₂O₂ + 2ROOH + NO_z). The sum H₂O₂ + ROOH is abbreviated as “perox” in the figure labels.

gen radicals. However, VOC are also important radical sources, so that O₃/S_H can be expected to decrease with increasing VOC. O₃/S_H can also vary photochemical age, since S_H here represents the summed source over the period of ozone production. The ratio O₃/NO_y (included in Figure 2b) is useful in this regard because it indirectly accounts for photochemical aging. O₃/NO_y can be viewed as O₃/NO_z multiplied by an aging term (NO_z/NO_y).

[30] As shown in Figure 1f, the ratio O₃/S_H decreases with increasing VOC emissions along the sensitivity transition. The change in O₃/S_H is proportional to the change in O₃/NO_z along the sensitivity transition, and thus explains much of the change in the transition value of O₃/NO_z from low to high emissions.

[31] As an alternative approach, it is possible to use difference ratios such as ΔO₃/ΔNO_z, where ΔO₃ and ΔNO_z represent differences relative to background values ((O₃-O_{3b}) and (NO_z-NO_{zb})). The difference ratio is related to the O₃-NO_z slope, which has been used to evaluate the ozone production efficiency per NO_x [Trainer *et al.*, 1993]. The difference ratio is related to Kleinman's S_H/L_N as follows:

$$\frac{\Delta O_3}{\Delta NO_z} = \left[\frac{S_H}{L_N} \right] \left[\frac{L_N}{\Delta NO_z} \right] \left[\frac{\Delta O_3}{S_H} \right] \quad (6b)$$

[32] The error term is now ΔO₃/S_H. This term can be interpreted as an ozone production efficiency per primary radical production [see Daum *et al.*, 2000a]. However, since the reaction sequence leading to production of radicals from secondary hydrocarbons is similar to the reaction sequence leading to production of O₃, it is possible to view ΔO₃/S_H as a ratio of two closely related photochemical processes. As such, this ratio is likely to show little variation over a wide range of photochemical conditions. The ratio ΔO₃/S_H is also related to the "chain length", the ratio of chain propagation to chain termination described by Tonnesen and Dennis [2000a], if chain propagation is viewed as being proportional to production of O₃.

[33] As shown in Figures 1g, 1h, and 2c, the ratios ΔO₃/ΔHNO₃, ΔO₃/ΔNO_z, and ΔO₃/ΔNO_y show a good correlation with NO_x-VOC sensitivity for O₃ below 250 ppb. The values of these ratios along the sensitivity transition still vary from low to high emissions. The correlation between these ratios and NO_x-VOC sensitivity becomes substantially worse for O₃ higher than 250 ppb, suggesting that these ratios may behave differently in highly polluted environments. The test ratio ΔO₃/S_H (Figure 1i) also remains nearly constant along the sensitivity transition for O₃ below 250 ppb, and decreases with increasing emissions for higher O₃. This ratio can also be interpreted as net ozone production efficiency per primary radical production (OPE_R) and compared with previous results from Daum *et al.* [2000]. Daum *et al.* reported OPE_R from 1 to 4, higher than the values shown here. However, Daum's values represent production only and do not include loss terms.

[34] The ratios O₃/(2H₂O₂ + NO_z) and O₃/(2H₂O₂ + 2ROOH + NO_z) are especially significant because they are directly related to the error terms in equation (6a). The relation can be expressed as follows:

$$\frac{O_3}{(2H_2O_2 + NO_z)} = \left[\frac{S_H}{(2H_2O_2 + NO_z)} \right] \left[\frac{O_3}{S_H} \right] \quad (7a)$$

or, in difference form

$$\frac{\Delta O_3}{\Delta(2H_2O_2 + NO_z)} = \left[\frac{S_H}{\Delta(2H_2O_2 + NO_z)} \right] \left[\frac{\Delta O_3}{S_H} \right] \quad (7b)$$

[35] Since H₂O₂ and NO_z represent the major radical sinks, the ratio S_H/(2H₂O₂ + NO_z) is determined almost entirely by the removal rate of H₂O₂ and NO_z. This is analogous to the term L_N/NO_z in equation (6a), which is determined by the removal rate of NO_z. The terms O₃/S_H and ΔO₃/S_H appear identically in equations (6a), (6b), (7a), and (7b). Thus, the ratios O₃/(2H₂O₂ + NO_z) and O₃/(2H₂O₂ + 2ROOH + NO_z) can be interpreted as a test for errors in the indicator ratio O₃/NO_z. Because they are associated with ΔO₃/S_H, these ratios can also be associated with ozone production efficiency per primary radical production and with chain length.

[36] As shown in Figures 1j and 2b, the ratios O₃/(2H₂O₂ + NO_z) and O₃/(2H₂O₂ + 2ROOH + NO_z) show patterns of variation that are very similar to O₃/S_H. Previous results from 3-D models and measurements [Sillman *et al.*, 1998] suggested that these ratios should have a near-constant value in photochemically aged air. The results here show a broader pattern of variation. The ratio tends to decrease with increasing O₃ along the sensitivity transition, and also decreases (though not consistently) with increasing VOC. The range of ratio values identified by Sillman *et al.* [1998] (O₃/(2H₂O₂ + NO_z) = 6–8) are comparable with the values shown in Figure 2c for the appropriate range of O₃ (80–140 ppb). The difference ratio ΔO₃/Δ(2H₂O₂ + 2ROOH + NO_z) (Figures 1k and 2c) shows a pattern of variation that is comparable to ΔO₃/S_H.

[37] Figure 2b shows a direct comparison between the values of O₃/NO_z, O₃/(2H₂O₂ + NO_z) and other similar ratios along the NO_x-VOC transition. As shown, these ratios all show a similar tendency to decrease as conditions range from relatively clean to highly polluted. This result is important because it suggests that O₃/(2H₂O₂ + NO_z) provides a measurement-based test for the NO_x-VOC transition value associated with the indicator ratios. The NO_x-VOC transition values for indicators represent model predictions and cannot be tested readily against measurements. Since O₃/(2H₂O₂ + NO_z) and O₃/(2H₂O₂ + 2ROOH + NO_z) are correlated to the indicator transition values but are not themselves correlated with NO_x-VOC sensitivity, they provide an indirect test for the transition values. A similar correlation is found for the difference ratios (Figure 2c).

[38] The behavior of O₃/NO_z at high VOC is also influenced by the increasingly dominant role of PAN and other organic nitrates. In contrast with HNO₃, the ratio O₃/PAN does not correlate with NO_x-VOC sensitivity (see Figure 1k) [see also Tonnesen and Dennis, 2000b]. At warm temperatures and relatively high NO_x (>0.5 ppb) PAN formation reaches an approximate steady state that is proportional to O₃, and the ratio O₃/PAN decreases with increasing VOC [see Sillman *et al.*, 1990]. The correlation between O₃/NO_z and NO_x-VOC sensitivity breaks down

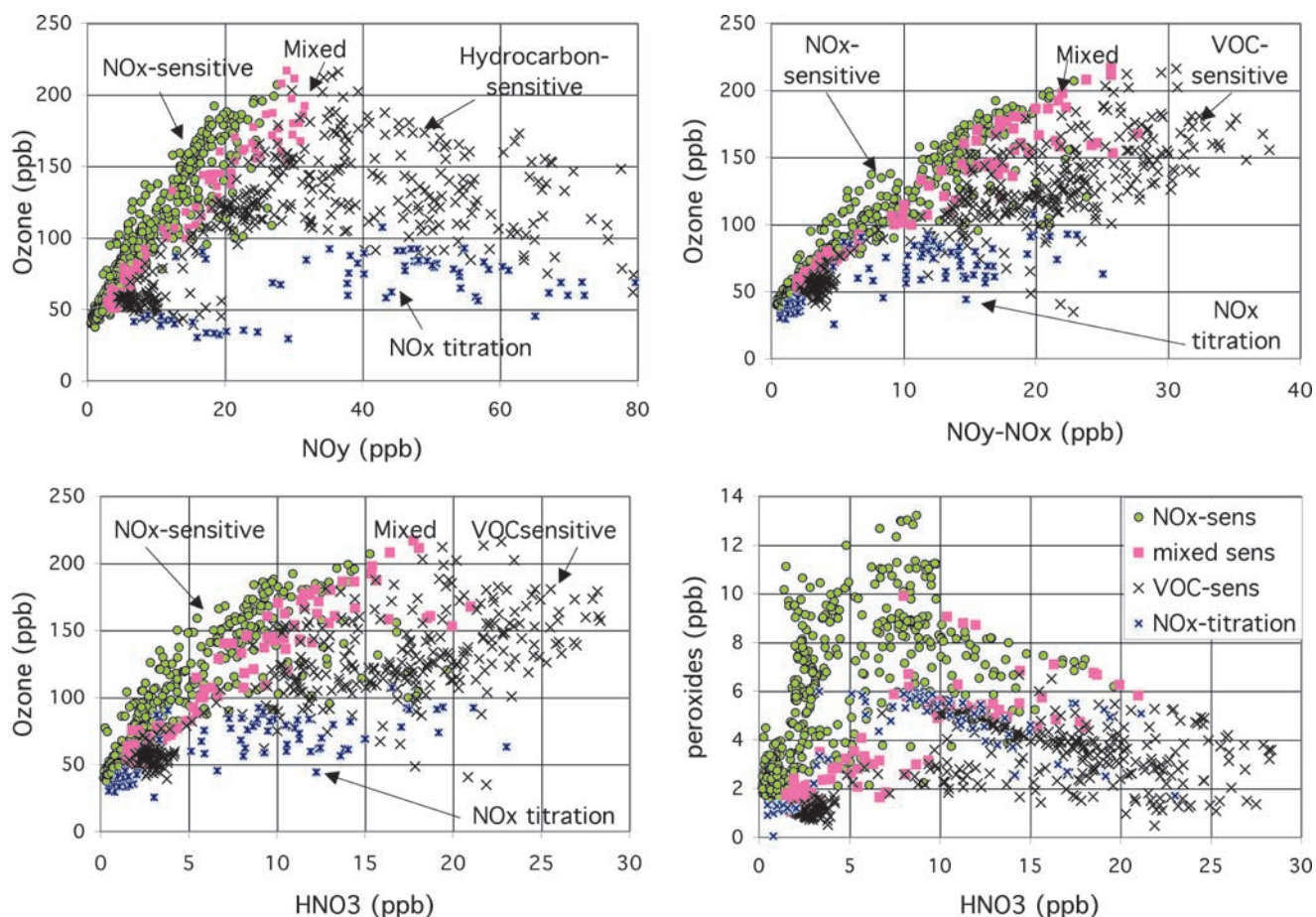


Figure 3. Correlations for (a) O₃ versus NO_y, (b) O₃ versus NO₂, (c) O₃ versus HNO₃, and (d) total peroxides versus HNO₃ (all in ppb) at 1500–1600 from the 3-D simulations listed in Table 1. Each location is classified as NO_x-sensitive (green circles), VOC-sensitive (crosses), mixed or with near-zero sensitivity (lavender squares), and dominated by NO_x titration (blue asterisks) based on definitions in the text.

when PAN and other organic nitrates become the dominant component of NO_z.

[39] In summary, several of the ratios previously identified by Sillman [1995] as NO_x-VOC indicators (especially O₃/NO_z and O₃/HNO₃) appear to show systematic variations in behavior as conditions vary from relatively clean to highly polluted. These variations can be understood conceptually if ratios are viewed as imperfect representations of the theoretical ratio S_H/L_N, which appears to correlate closely with NO_x-VOC sensitivity both in these 0-D calculations and in previous work by Kleinman *et al.* [1997]. Variations in the behavior of indicator ratios in models is also associated with predicted variations in the ratios O₃/(2H₂O₂ + NO₂) and O₃/(2H₂O₂ + 2ROOH + NO₂), which might be compared with ambient measurements. The next section shows equivalent results from 3-D models.

5. Results From 3-D Calculations

[40] Figure 3 shows O₃ versus NO_z (afternoon values at the surface) from a composite of 3-D simulations (see summary in Table 1). The simulations include a series of regional-scale simulations in the eastern U.S. (with horizontal extent 1000 km or larger and horizontal resolution 20

× 20 km or 5 × 5 km) and for the San Joaquin valley (California), and urban-scale simulations (with horizontal extent 150–250 km) for Atlanta and Los Angeles. The figure includes results from a modified form of the simulation from Lu and Chang [1998] [see Sillman *et al.*, 2001], which included results that contradicted the original analysis of indicator ratios by Sillman [1995]. Results represent afternoon hours (1500–1600 LST).

[41] The figure also shows predicted NO_x-VOC sensitivity for each location, based on differences between O₃ in each model base case and in equivalent scenarios with 25% or 35% reductions in anthropogenic VOC and in NO_x. Locations have been classified according to the following definitions:

1. *NO_x-sensitive*: O₃ in the scenario with reduced NO_x is lower than O₃ in both the base case and in the scenario with reduced VOC at the specified location and hour by at least 5 ppb.

2. *VOC-sensitive*: O₃ in the scenario with reduced VOC is lower than O₃ in both the base case and in the scenario with reduced NO_x by at least 5 ppb.

3. *Mixed*: The scenarios with reduced NO_x and reduced VOC have O₃ within 5 ppb of each other, and both have O₃ lower than in the base case by at least 5 ppb.

4. *NO_x-titration*: O₃ in the scenario with reduced NO_x is larger than O₃ in the base case by at least 5 ppb, and O₃ in the simulation with reduced VOC is not lower by 5 ppb or more relative to the base case.

[42] All other locations are viewed as insensitive to NO_x and VOC in the context of the model domain. These typically represent locations with O₃ dominated by transport from outside the model boundary rather than calculated photochemical production.

[43] The locations dominated by NO_x-titration are usually near large sources of NO. These locations typically have relatively low O₃, and O₃ has been affected primarily by the reaction $O_3 + NO \rightarrow NO_2$ in the presence of directly emitted NO rather than by ozone production chemistry. Indicator ratios in these locations can be misleading because the indicator ratios involve photochemical reaction products associated with ozone formation rather than removal. Evaluation of indicator ratios will be based on the ability to distinguish between NO_x-sensitive and VOC-sensitive ozone production, ignoring the locations dominated by NO_x-titration.

[44] As shown in Figure 3, NO_x-sensitive and VOC-sensitive locations are associated with a different range of values in the correlation plots for O₃ versus NO_y and other ratios. The mixed locations occupy intermediate values between the NO_x-sensitive and VOC-sensitive locations. Results for peroxides versus HNO₃ are especially useful for identifying NO_x-VOC sensitivity because there is a large difference between model values associated with NO_x-sensitive and VOC-sensitive locations. For O₃/NO_y, O₃/NO_z and O₃/HNO₃ the difference between NO_x-sensitive and VOC-sensitive locations is smaller and therefore more likely to be affected by model uncertainties. Also, locations dominated by NO_x titration cannot be distinguished from other locations based on peroxides versus HNO₃, because the process of NO_x titration has little impact on peroxides or HNO₃. NO_x-titration locations are clearly identifiable in the plot of O₃ versus NO_y.

[45] Previously *Sillman* [1995] associated NO_x-sensitive and VOC-sensitive conditions with high and low values of indicator ratios (O₃/NO_y, etc.) and identified transition values that separated NO_x-sensitive and VOC-sensitive locations (O₃/NO_y = 6–8, O₃/NO_z = 8–10, O₃/HNO₃ = 12–15). A careful examination of Figure 3 shows that the NO_x-VOC transition does not correspond exactly to these transition values, and that the transition values of indicator ratios decreases with increasing O₃. The change in indicator transition values is especially noticeable for O₃ less than 80 ppb (with NO_x-VOC transitions at O₃/NO_y = 11–15, O₃/NO_z = 15–20). For O₃ greater than 100 ppb the NO_x-VOC transition corresponds to the ratio values previously identified by *Sillman* [1995]. By contrast, NO_x-VOC transition for ratios involving peroxides (H₂O₂/HNO₃ = 0.2–0.3; total peroxides/HNO₃ = 0.3–0.45) do not appear to vary for the range of clean and polluted conditions shown here.

[46] Figure 4 shows the same results in different format, with the indicator ratio O₃/NO_y plotted versus O₃ for NO_x-sensitive and VOC-sensitive locations. This variation in transition ratios in Figures 3 and 4 is broadly consistent with the indicator transition values identified from the 0-D simulations (see Figure 2).

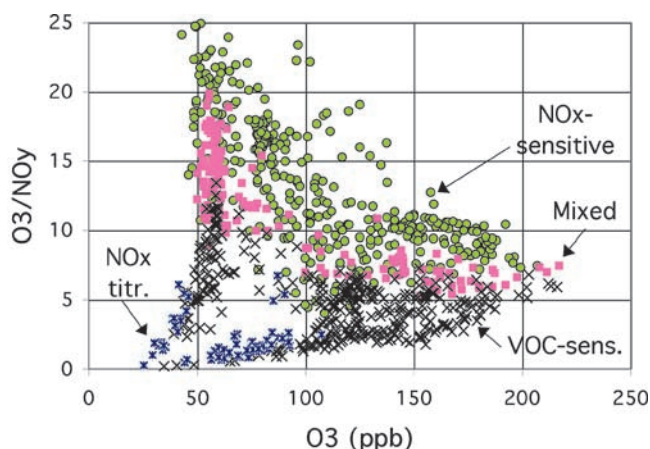


Figure 4. O₃/NO_y versus O₃ in the 3-D simulations listed in Table 1, with locations classified as NO_x-sensitive (green circles), VOC-sensitive (crosses), mixed or with near-zero sensitivity (lavender squares), and dominated by NO_x titration (blue asterisks).

[47] From Figure 3 it appears that the NO_x-VOC transition might fit more closely to an indicator ratio of the form $\Delta O_3/\Delta NO_y$, where ΔO_3 represents the difference between O₃ at the location in question and the model background O₃ (40 ppb). Indicator ratios of the form $\Delta O_3/\Delta NO_y$ would also be advantageous for evaluating NO_x-VOC sensitivity in specific urban areas that include significant transport of O₃ from upwind. As pointed out by *Dommen et al.* [1999] measured indicator values in plumes from relatively small cities reflect NO_x-VOC sensitivity associated with region-wide production of O₃ rather than the impact of emissions in the individual urban center. Indicators with the form $\Delta O_3/\Delta NO_y$ could provide information about individual metropolitan area emissions as well as region-wide conditions. However, determination of background values provides an additional uncertainty for indicators with this form.

[48] In order to identify background concentrations to be used in forming these ratios, the following formalism will be used: background concentrations will be based on the model grid with minimum NO_y over the relevant portion of the model domain at the hour of interest. Here, we assume that the region of interest might be either (1) an urban plume surrounded by “background” rural concentrations; or (2) a polluted region (such as the eastern half of the U.S.) with well defined upwind conditions. We also assume that there is a specified (afternoon) hour of interest, at a time when surface conditions reflect photochemical production of O₃ in a well-mixed layer. Background concentrations will be set equal to conditions in the model grid with minimum NO_y at the same hour and for a specified altitude. The location with minimum NO_y is selected based on a horizontal domain that includes the rural background region surrounding the plume or polluted region. As suggested by *Blanchard and Stoeckenius* [2001], the model impact of reduced NO_x and VOC predicted for the location with minimum NO_x is subtracted from the model impact of reduced NO_x and VOC at other locations, so that the analysis will not include sensitivity to emissions upwind of the boundary point. Although somewhat arbitrary, this

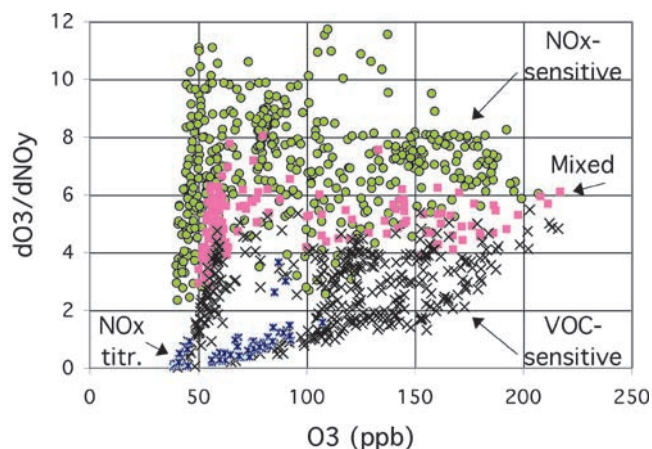


Figure 5. $\Delta O_3/\Delta NO_y$ versus O_3 in the 3-D simulations listed in Table 1, with locations classified as NO_x-sensitive (green circles), VOC-sensitive (crosses), mixed or with near-zero sensitivity (lavender squares), and dominated by NO_x titration (blue asterisks). ΔO_3 and ΔNO_y refer to differences relative to background values.

method is advantageous because the same ratios and equivalent background values can easily be determined from a network of measurements that includes samples within an urban plume and the surrounding rural region. It also avoids the use of morning values to determine background, because these values are influenced by the nocturnal boundary layer and uncertain rates of entrainment from aloft. We have also avoided using the O₃-NO₂ slope, which is often reported for measured data sets, because the value of this slope is often unclear and may depend on the precise location of the measurements.

[49] The $\Delta O_3/\Delta NO_y$ and other ratios defined in this manner provide specific values at each model location (or at each measurement site) other than the site identified as the rural background. In the subsequent analysis we will use the above formalism to define background values for urban and regional subdomains of individual model scenarios. The model indicator ratios based on these background values will be compared with the predicted impact of reduced NO_x and VOC emissions within the equivalent subdomain.

[50] As shown in Figure 5, the ratio $\Delta O_3/\Delta NO_y$ is strongly correlated with NO_x-VOC sensitivity for the group of 3-D simulations included here. There is some overlap between NO_x-sensitive and VOC-sensitive locations, with NO_x-sensitive values as low as 3 and VOC-sensitive values as high as 5. The NO_x-VOC transition value appears to be similar for locations with high and low O₃, although the value of $\Delta O_3/\Delta NO_y$ for O₃ below 60 ppb is especially sensitive to the assumed background value.

[51] The information in Figure 5 can be conveniently summarized and evaluated by reporting the distribution of ratio values associated with NO_x-sensitive and VOC-sensitive locations. In Figure 5 the indicator values for VOC-sensitive locations are lower than values for NO_x-sensitive locations, and there is little overlap between the ranges of values. Locations with mixed sensitivity typically have intermediate indicator values. As was done in *Sillman et al.* [1998] the indicator results for individual simulations are summarized by recording the 5th, 50th and 95th percentile

indicator values for NO_x-sensitive and VOC-sensitive locations. A NO_x-VOC indicator is successful if the 95th percentile value for VOC-sensitive locations is equal to or less than the 5th percentile value for NO_x-sensitive locations, and if the transition values remain similar in models for different locations and assumptions. These 95th percentile and 5th percentile values identify the transition from NO_x-sensitive to VOC-sensitive conditions.

[52] As shown in Table 2, the ratios $\Delta O_3/\Delta NO_y$, $\Delta O_3/\Delta NO_z$ and $\Delta O_3/\Delta HNO_3$ (where HNO₃ is interpreted to include aerosol nitrate) are potentially useful as NO_x-VOC indicators. These ratios are correlated with NO_x-VOC sensitivity both at the regional scale and within urban subsets of model domains, with ΔO_3 , etc. relative to the appropriate background for the subdomain. Median values of the ratios for NO_x-sensitive locations are often twice as high as median values for VOC-sensitive locations, and the 95th percentile VOC-sensitive value and 5th percentile NO_x-sensitive value are generally comparable. Ratio values at the NO_x-VOC transition are: $\Delta O_3/\Delta NO_y = 4-6$; $\Delta O_3/\Delta NO_z = 5-7$; and $\Delta O_3/\Delta HNO_3 = 8-10$. It is noteworthy that range of values from the model for San Joaquin reported by *Lu and Chang* [1998] are generally comparable to the others. Results for O₃/NO_z from this model differed sharply from the indicator results in *Sillman* [1995], probably because the scenario reported by San Joaquin had different boundary conditions [see *Sillman et al.*, 2001]. When ratios such as $\Delta O_3/\Delta NO_y$ along with the described procedure for identifying background values are used, model boundary conditions are less important.

[53] Although the ratios $\Delta O_3/\Delta NO_y$, etc. effectively separate NO_x-sensitive and VOC-sensitive conditions for many of the 3-D simulations, there were some situations with ambiguous results. The ratios $\Delta O_3/\Delta NO_z$ and $\Delta O_3/\Delta HNO_3$ performed poorly in the models for Los Angeles, San Joaquin and in one Nashville case. In the ambiguous cases, the 5th percentile ratio value for NO_x-sensitive locations is comparable to the median value for VOC-sensitive locations, suggesting significant overlap of values between NO_x-sensitive and VOC-sensitive conditions. Performance is significantly better for $\Delta O_3/\Delta NO_y$ in these locations. Indicator results are especially poor for the model for Los Angeles reported by *Chock et al.* [1999]. Transition values can also be shifted by 20% in response to changes in dry deposition rates.

[54] Table 2 also includes results for the original indicator ratios (O₃/NO_y, H₂O₂/HNO₃, etc.) from *Sillman* [1995]. These ratios generally show a larger separation between NO_x-sensitive and VOC-sensitive locations than the ratios with the form $\Delta O_3/\Delta NO_y$, etc. They also avoid the uncertainty associated with background values for $\Delta O_3/\Delta NO_y$. As described above, the NO_x-VOC transition for the ratios O₃/NO_y, O₃/NO_z and O₃/HNO₃ are much higher in the models for San Joaquin and in the model for Los Angeles reported by *Chock et al.* than in other cases.

[55] The ratio H₂O₂/HNO₃ and similar ratios involving summed peroxides generally show the strongest correlation with NO_x-VOC sensitivity and the smallest variation among individual models. However, the difference ratio relative to background ($\Delta H_2O_2/\Delta HNO_3$) does not correlate with NO_x-VOC sensitivity. Typically, H₂O₂ is lower inside an urban plume relative to the surrounding rural area [*Weinstein-*

Table 2. Distribution of Indicator Values for NO_x- and VOC-Sensitive Locations in 3-D Simulations

Indicator	VOC-Sensitive Locations			NO _x -Sensitive Locations		
	5th Percentile	50th Percentile	95th Percentile	5th Percentile	50th Percentile	95th Percentile
			$\Delta O_3/\Delta NO_y$			
Nashville, full domain	0.4	2.9	3.6	3.4	4.7	5.3
Nashville, high deposition ^a	0.3	3.5	4.3	4.6	6.7	7.7
Nashville, urban subdomain	1.0	2.5	3.6	4.2	5.6	12.4
Northeast, full domain	2.8	4.0	4.8	5.7	7.7	9.0
Northeast, urban subdomain	1.8	3.8	5.0	5.0	6.5	7.2
Lake Michigan	2.4	3.4	4.3	3.5	6.2	7.6
Atlanta	1.6	2.8	4.5	4.5	6.9	11.1
San Joaquin (Sillman)	0.6	2.8	4.9	4.4	7.5	11.4
San Joaquin (Lu and Chang)	1.3	3.2	4.2	3.6	8.4	32.4
Los Angeles (Godowitch)	0.9	2.3	4.6	5.2	7.9	11.9
Los Angeles (Chock)	0.6	3.7	6.0	3.5	8.6	13.7
			$\Delta O_3/\Delta NO_2$			
Nashville, full domain	1.2	3.6	5.0	3.8	5.3	6.1
Nashville, high deposition ^a	1.6	4.8	6.6	5.3	8.1	9.1
Nashville, urban subdomain	1.9	4.0	5.0	5.1	7.1	15.4
Northeast, full domain	4.7	5.0	5.6	6.7	8.5	9.9
Northeast, urban subdomain	2.8	4.4	5.4	5.7	7.4	8.3
Lake Michigan	3.0	4.0	5.2	5.7	7.3	8.5
Atlanta	3.6	4.5	5.9	6.1	9.2	14.6
San Joaquin (Sillman)	2.4	6.1	8.1	6.0	9.9	15.2
San Joaquin (Lu and Chang)	3.5	6.4	6.6	5.0	11.6	31.4
Los Angeles (Godowitch)	3.0	4.5	6.3	6.2	9.0	15.6
Los Angeles (Chock)	4.2	6.7	10.0	8.3	10.9	16.6
			$\Delta O_3/\Delta HNO_3$			
Nashville, full domain	1.4	4.2	6.5	4.6	6.7	8.2
Nashville, high deposition ^a	1.8	5.9	9.4	7.1	11.5	14.1
Nashville, urban subdomain	2.2	5.1	7.9	8.0	12.8	40.3
Northeast, full domain	7.3	8.4	10.7	11.0	15.6	23.9
Northeast, urban subdomain	4.9	8.4	11.4	13.1	27.3	235.7
Lake Michigan	3.6	4.8	7.6	8.8	12.5	18.2
Atlanta	4.1	5.3	7.3	7.3	13.1	20.5
San Joaquin (Sillman)	2.7	7.4	11.0	9.4	14.7	29.6
Los Angeles (Godowitch)	3.5	5.5	8.9	9.1	14.6	31.2
Los Angeles (Chock)	6.2	10.1	25.3	13.1	18.3	42.4
			O_3/NO_y			
Nashville	2.2	3.6	5.6	7.1	10.8	13.
Nashville, high dep. ^a	2.6	5.3	7.2	8.7	13.9	17.
Northeast corridor	5.0	5.4	6.5	8.2	12.7	18.
Lake Michigan	3.5	5.2	6.6	7.2	11.7	16.
Atlanta	3.6	5.1	7.2	8.1	14.3	27.
Los Angeles (Godowitch)	1.4	3.2	6.0	7.2	10.4	20.
Los Angeles (Chock)	1.0	5.4	9.1	5.9	18.	24.
San Joaquin (Sillman)	3.0	7.3	11.6	15.	26.	56.
San Joaquin (Chang)	5.4	7.7	12.3	12.5	22.	52.
			O_3/NO_2			
Nashville	5.3	6.3	7.3	8.4	12.4	13.
Nashville, high dep. ^a	7.0	8.8	9.9	10.5	16.8	20.
Northeast corridor	6.7	7.1	7.7	9.7	14.4	20.
Lake Michigan	4.5	5.8	8.1	11.2	15.3	18.
Atlanta	7.1	8.6	10.0	11.9	17.7	33.
Los Angeles (Godowitch)	4.6	6.2	8.4	8.7	12.0	25.
Los Angeles (Chock)	6.2	10.	15	14.	23.	31.
San Joaquin (Sillman)	11.	16.	19.	21.	35.	73.
San Joaquin (Chang)	14.	16.	20.	17.	32.	68.
			O_3/HNO_3			
Nashville	6.	8.	9.	12.	19.	21.
Nashville, high dep. ^a	8.	11.	14.	15.	25.	29.
Northeast corridor	10.	11.	16.	17.	27.	42.
Lake Michigan	5.	7.	11.	16.	28.	39.
Atlanta	8.	10.	13.	15.	25.	54.
Los Angeles (Godowitch)	5.	8.	12.	13.	19.	50.
Los Angeles (Chock)	9.	15.	40.	23.	39.	80.
San Joaquin (Sillman)	14.	20.	28.	27.	54.	155.

Table 2. (continued)

Indicator	VOC-Sensitive Locations			NO _x -Sensitive Locations		
	5th Percentile	50th Percentile	95th Percentile	5th Percentile	50th Percentile	95th Percentile
	<i>H₂O₂/HNO₃</i>					
Nashville	0.11	0.18	0.23	0.30	0.64	0.82
Nashville, high dep. ^a	0.09	0.15	0.21	0.26	0.55	0.70
Northeast corridor	0.22	0.33	0.40	0.68	1.58	3.1
Lake Michigan	0.03	0.13	0.24	0.37	1.15	1.8
	<i>(H₂O₂+ ROOH)/HNO₃</i>					
Nashville	0.18	0.23	0.31	0.39	0.73	1.01
Nashville, high dep. ^a	0.22	0.28	0.37	0.54	1.14	1.48
Northeast corridor	0.22	0.39	0.54	0.93	2.0	4.3
Lake Michigan	0.06	0.20	0.32	0.49	1.6	2.6
Atlanta ^b	0.17	0.27	0.55	0.55	1.44	4.5
Los Angeles (Godowitch) ^b	0.06	0.22	0.41	0.40	0.87	2.8
Los Angeles (Chock) ^b	0.12	0.33	1.8	0.80	2.2	4.4
San Joaquin (Sillman) ^b	0.24	0.38	0.56	1.0	2.7	8.7
San Joaquin (Chang) ^b	0.17	0.23	0.52	0.72	1.8	6.3
	<i>H₂O₂/NO_z</i>					
Nashville	0.12	0.15	0.19	0.21	0.41	0.45
Nashville, high dep. ^a	0.10	0.13	0.17	0.18	0.37	0.41
Northeast corridor	0.14	0.20	0.21	0.36	0.80	1.4
Lake Michigan	0.03	0.10	0.19	0.27	0.60	0.87
	<i>(H₂O₂+ ROOH)/NO_z</i>					
Nashville	0.13	0.20	0.27	0.29	0.59	0.85
Nashville, high dep. ^a	0.15	0.22	0.30	0.35	0.79	1.08
Northeast corridor	0.14	0.24	0.28	0.49	1.10	1.91
Lake Michigan	0.05	0.15	0.26	0.35	0.81	1.22
Atlanta ^b	0.14	0.23	0.44	0.42	1.04	2.8
Los Angeles (Godowitch) ^b	0.05	0.17	0.33	0.26	0.55	1.4
	<i>H₂O₂/NO_y</i>					
Nashville	0.05	0.09	0.12	0.17	0.36	0.42
Nashville, high dep. ^a	0.04	0.07	0.10	0.14	0.32	0.40
Northeast corridor	0.11	0.14	0.17	0.30	0.68	1.3
Lake Michigan	0.02	0.09	0.16	0.22	0.43	0.78
	<i>(H₂O₂+ ROOH)/NO_y</i>					
Nashville	0.08	0.12	0.18	0.24	0.52	0.98
Nashville, high dep. ^a	0.08	0.12	0.17	0.28	0.68	1.15
Northeast corridor	0.11	0.19	0.22	0.38	0.9	1.72
Lake Michigan	0.04	0.12	0.25	0.28	0.58	1.09
Atlanta ^b	0.10	0.12	0.19	0.29	0.83	2.2
Los Angeles (Godowitch) ^b	0.02	0.08	0.19	0.22	0.47	1.2

The table shows 5th, 50th, and 95th percentile indicator values (with percentile ordering by indicator value) for VOC-sensitive locations and NO_x-sensitive locations as defined in the text. The terms ΔO₃, ΔNO_y, ΔNO_z and ΔHNO₃ represent the difference between values at specified locations and background values. In some cases results are shown separately for (a) the full model domain and (b) an urban subdomain. In these cases NO_x-VOC sensitivity is defined relative to changed emissions within the model subdomain and background values are determined relative to the same subdomain. Models are described in Table 1.

^aThe Nashville high-deposition scenario has dry deposition rates of 5 cm² s⁻¹ for H₂O₂ and HNO₃, as opposed to 2.5 cm² s⁻¹ in the standard scenario.

^bIn models with CB-4 chemistry, “H₂O₂” is interpreted as a surrogate for the sum of H₂O₂ and organic peroxides.

Lloyd *et al.*, 1998]. This decrease in H₂O₂ may suggest that the urban plume has VOC-sensitive chemistry, but it may also occur because the surrounding rural area has strongly NO_x-sensitive conditions. A correlation with urban NO_x-VOC chemistry independent of conditions in the surrounding rural region does not appear to be possible. H₂O₂/HNO₃ and similar ratios correlate with NO_x-VOC sensitivity on regional scales, where most of the H₂O₂ and HNO₃ has been produced within the model domain of interest.

6. Discussion

[56] The results of the previous section should be viewed in the context of the need to identify the range of conditions for which the proposed NO_x-VOC indicators are valid. The

general pattern of correlation between indicators and NO_x-VOC sensitivity appears to apply for a very wide range of conditions, as illustrated in Figures 3 and 4. As pointed out by Lu and Chang [1998], the NO_x-VOC transition values for some indicator ratios can vary significantly. However, this does not appear to be just a random variation among different models or locations. Rather, it is part of a systematic variation from relatively clean to highly polluted conditions, which is imperfectly captured by the indicator ratios. This variation can be explained in terms of the radical chemistry that drives the split into NO_x-sensitive and VOC-sensitive conditions.

[57] The indicator transition values from Sillman [1995] and Sillman *et al.* [1998] appear to be valid for moderately polluted conditions with O₃ from 80 to 200 ppb. The 0-D

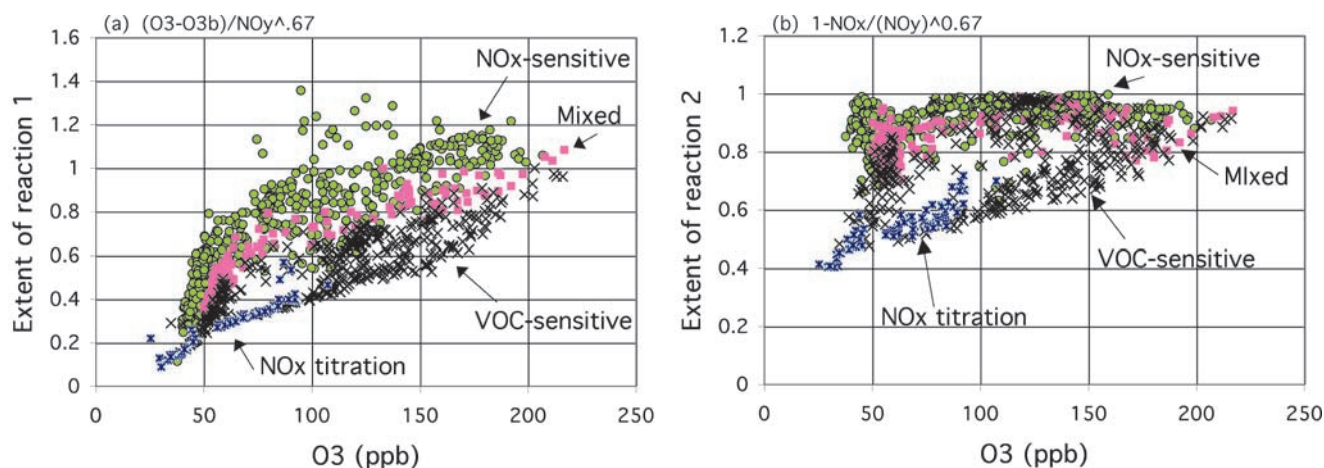


Figure 6. Extent of reaction parameters [Blanchard *et al.*, 1999] versus O₃ in the 3-D simulations listed in Table 1, with locations classified as NO_x-sensitive (green circles), VOC-sensitive (crosses), mixed or with near-zero sensitivity (lavender squares), and dominated by NO_x titration (blue asterisks). The extent parameters are (a) based on $\Delta O_3/\Delta NO_y^{0.67}$ (equation (8a)) and (b) based on $(NO_x/NO_y)^{0.67}$ (equation (8b)).

calculations shown here suggest that some indicator ratios (O₃/NO_z) may not be applicable for more highly polluted conditions, and others may have different NO_x-VOC transition values. This finding is especially important in connection to investigations of the chemistry of ozone formation in Mexico City. Sosa *et al.* [2000] reported that the ratio O₃/NO_z did not correlate well with NO_x-VOC sensitivity in 3-D models for Mexico City.

[58] From the calculations shown here, the indicator ratios involving peroxides appear to be more robust than the ratios involving O₃. Lu and Chang [1998] and Chock *et al.* [1999] reported transition values for H₂O₂/HNO₃ that differed from previously reported results.

[59] It may be possible to derive more robust ratios by using the form $\Delta O_3/\Delta NO_z$ rather than the simpler O₃/NO_z. Indicator ratios of this form are more consistent with the pattern of variation among NO_x-sensitive and VOC-sensitive locations shown in Figure 3. However, this would introduce additional uncertainty concerning the value of the background concentrations, which are needed to determine ΔO_3 . In addition, ratios with this form still show significant variation and in models for different locations. It is perhaps more useful to interpret measured indicator ratios by directly comparing correlations with the broad pattern of NO_x-VOC variation in Figure 3. A direct comparison of correlation plots would also help to establish the validity of using specific sets of measurements in combination with these theoretical results.

[60] It is useful to compare indicator ratios described here with the “extent-of-reaction” parameters developed by Johnson *et al.* [1990] and Blanchard *et al.* [1999; Blanchard and Stoeckenius, 2001] [see also Olzyna *et al.*, 1994; T. Chang *et al.*, 1997]. Extent-of-reaction parameters were derived from smog chamber experiments, and are based on the finding that ozone in photochemically aged air is sensitive to NO_x while ozone in air with relatively unprocessed emissions is sensitive to VOC. Although the rationale is different, the extent-of-reaction parameters are often similar to the ratio $\Delta O_3/\Delta NO_y$ used here. Blanchard *et al.* [1999] developed the following parameters for extent of

reaction (modified here to account for dry deposition of NO_y):

$$\text{Extent}_1 = \frac{1.1O_3 - O_3b - NO + 1.23 NO_y}{22NO_y^{0.67}} \quad (8a)$$

$$\text{Extent}_2 = \left[1 - \frac{NO_x}{1.3NO_y} \right]^{0.67} \quad (8b)$$

[61] Figure 6 shows how the extent parameters vary for NO_x-sensitive and VOC-sensitive locations for the ensemble of models used here. The first extent parameter (based on $\Delta O_3/\Delta NO_y^{0.67}$) effectively separates NO_x-sensitive from VOC-sensitive locations, but the NO_x-VOC transition tends to vary from low to high O₃. A better correlation with NO_x-VOC sensitivity would be obtained using the original extent parameter developed by Johnson *et al.* [1990] (based on $\Delta O_3/\Delta NO_y$), although the original parameter would need to be modified to account for removal of NO_y by dry deposition. Blanchard *et al.* [1999] described how the 0.67 exponent was added based on results from 0-D calculations and smog chamber experiments. Based on the isopleths in Figure 1h and 2b, it is possible that the form $\Delta O_3/\Delta NO_y^{0.67}$ may be more appropriate for highly polluted environments. The NO_x-VOC transition in the isopleth plots (see Figure 2b) correlates more closely to $\Delta O_3/\Delta NO_y^{0.67}$ than to $\Delta O_3/\Delta NO_y$ for highly polluted conditions (O₃ > 150 ppb).

[62] The second extent parameter (based on $1-NO_x/NO_y$) is loosely correlated with NO_x-VOC sensitivity but there are a large number of exceptions, with VOC-sensitive chemistry and extent of reaction close to 1. A similar analysis was done by Blanchard and Stoeckenius [2001]. We also found poor performance for a third extent parameter, reported by Blanchard *et al.* [1999], based on O₃ and NO_x. The poor correlation for this parameter may be related to a flaw in the extent-of-reaction concept. Figure 7 shows isopleths for NO_x/NO_y in comparison with O₃ from the 0-D calculations (equivalent to Figure 1). As shown in the figure, high NO_x/

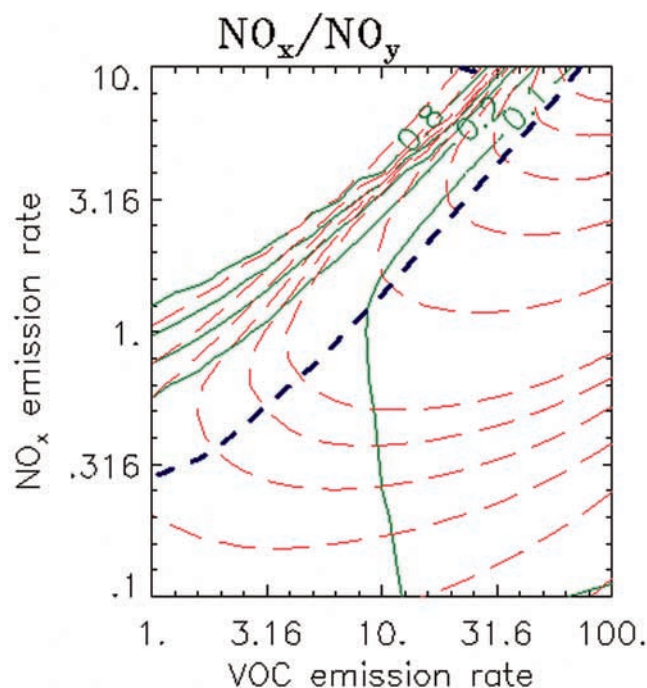


Figure 7. Isopleths for NO_x/NO_y (red dashed lines) as a function of NO_x and VOC emissions (10^{12} molec. cm^{-2} s^{-1}) in 0-D simulations, as in Figure 1. The solid green line represents O_3 , and the blue dashed line represents the transition from VOC-sensitive to NO_x -sensitive conditions.

NO_y ratios are associated with strongly VOC-sensitive chemistry in which ozone production is sharply limited by excess NO_x . The high NO_x/NO_y also corresponds to $S_{\text{H}}/S_{\text{N}} < 1$ in Figure 1a. Low NO_x/NO_y ratios in Figure 7 correspond both to NO_x -sensitive conditions and to VOC-sensitive conditions that have relatively high rates of ozone production. In the 3-D simulations also a low value of the extent parameter (corresponding to high NO_x/NO_y) is associated with strongly VOC-sensitive chemistry, but a high value (corresponding to low NO_x/NO_y) can be associated with either NO_x -sensitive or VOC-sensitive conditions. The exceptional VOC-sensitive cases occur mainly in the simulation for Lake Michigan, in which a strongly VOC-sensitive plume from Chicago moves downwind and remains sensitive to VOC even after it ages. The extent-of-reaction parameters based on $\Delta\text{O}_3/\Delta\text{NO}_y$ show a closer correlation with NO_x -VOC sensitivity in models, possibly because $\Delta\text{O}_3/\Delta\text{NO}_y$ is associated with Kleinman's radical ratio ($S_{\text{H}}/L_{\text{N}}$, discussed in sections 2 and 4) rather than just the photochemical age.

7. Conclusion

[63] The above analysis has resulted in the following new findings concerning the use of secondary species NO_x -VOC indicators.

1. The behavior of some proposed indicator ratios tends to be different for relatively clean environments ($\text{O}_3 < 80$ ppb), moderately polluted (100–200 ppb O_3) and highly polluted environments ($\text{O}_3 > 200$ ppb). This is especially true for O_3/NO_z . Previously reported results from Sillman [1995] and Sillman *et al.* [1998] were based on moderately polluted conditions.

2. The correlation with NO_x -VOC sensitivity is stronger and more consistent for ratios involving peroxides ($\text{H}_2\text{O}_2/\text{HNO}_3$, etc.) than for ratios such as O_3/NO_z .

3. The ratios $\text{O}_3/(2\text{H}_2\text{O}_2 + \text{NO}_z)$ and $\text{O}_3/(2\text{H}_2\text{O}_2 + 2\text{ROOH} + \text{NO}_z)$ should also vary from clean to highly polluted environments. These ratios provide a measurement-based test of indicator NO_x -VOC transition values.

4. Indicator ratios with the form $\Delta\text{O}_3/\Delta\text{NO}_y$ (where ΔO_3 and ΔNO_y represents the difference between values at a specific location and background values) are proposed for evaluating local NO_x -VOC sensitivity in urban plumes with well-defined background concentrations. This ratio is generally correlated with O_3 - NO_x -VOC sensitivity in models, but there is significant variation among models for different locations.

5. Variations in indicator behavior are analytically linked to variations in the ozone production efficiency per primary radical production (O_3/S_{H}).

6. The “extent-of-reaction” parameter ($\Delta\text{O}_3/\Delta\text{NO}_y^{0.67}$) also correlates with NO_x -VOC sensitivity in models, but its behavior shows a systematic variation with O_3 . Extent parameters based on NO_x/NO_y do not correlate with model NO_x -VOC sensitivity.

[64] The indicator ratios discussed here are a potentially useful method for identifying NO_x -sensitive and VOC-sensitive conditions in the ambient atmosphere, but they are also subject to many uncertainties. These include: uncertain dry deposition rates, wet deposition, aerosol interactions, measurement error, and case-to-case variations. It is especially important to recognize that many of the results shown here depend on the mechanism used to represent photochemistry. Derived ratios such as the ozone production per primary radical production may depend on the detailed representation of reaction sequences of VOC, which are often highly parameterized. It is important to compare these values for different photochemical representations and compare them with measurements (including both smog chamber experiments).

[65] Perhaps the biggest weakness is the difficulty in testing the predicted indicator- NO_x -VOC relationship against ambient measurements. Comparisons between measured data sets and the predicted patterns of correlation in Figure 3 are likely to be more useful in establishing the validity of indicator ratios.

8. Notation

NO_z	NO_x reaction products, or NO_y - NO_x
S_{H}, Q	summed source of odd hydrogen radicals, including OH, HO_2 and RO_2 [referred to as Q in Kleinman <i>et al.</i> , 1997].
S_{N}	summed source of NO_x .
L_{N}	summed rate of photochemical removal of NO_x , also equal to the rate of production of NO_z .
OPE_{N}	ozone production efficiency per NO_x .
OPE_{R}	ozone production efficiency per primary radical production.

[66] **Acknowledgments.** Support for this research was provided by the National Science Foundation under grant #ATM-9713567 and by the U.S. Environmental Protection Agency under grant #F001046. Although the research described in this article has been funded by NSF and EPA, it

has not been subjected to peer and administrative review by either agency, and therefore may not necessarily reflect the views of the agencies, and no official endorsement should be inferred.

References

- Blanchard, C. L., and T. Stoeckenius, Ozone response to precursor controls: Comparison of data analysis methods with the predictions of photochemical air quality simulation models, *Atmos. Environ.*, **35**, 1203–1216, 2001.
- Blanchard, C. L., F. W. Lurmann, P. M. Roth, H. E. Jeffries, and M. Korc, The use of ambient data to corroborate analyses of ozone control strategies, *Atmos. Environ.*, **33**, 359–368, 1999.
- Carter, W. P. L., 2000. *Documentation of the SAPRC-99 chemical mechanism for VOC reactivity assessment*, final report, 00-AP-RT17-001-FR, Calif. Air Resour. Board, May 8, 2000.
- Chang, J. S., S. Jin, Y. Li, M. Beauharnois, C.-H. Lu, H.-C. Huang, S. Tanrikulu, and J. DaMassa, The SARMAP air quality model, final report, Air Resour. Board, Calif. Environ. Prot. Agency, Sacramento, 1997.
- Chang, T. Y., D. P. Chock, B. I. Nance, and S. L. Winkler, A photochemical extent parameter to aid ozone air quality management, *Atmos. Environ.*, **31**, 2287–2294, 1997.
- Chock, D. P., T. Y. Chang, S. L. Winkler, and B. I. Nance, The impact of an 8 h ozone air quality standard on ROG and NO_x controls in Southern California, *Atmos. Environ.*, **33**, 2471–2486, 1999.
- Daum, P. H., L. Kleinman, D. G. Imre, L. J. Nunnermacker, Y. N. Lee, S. R. Springston, and L. Newman, Analysis of the processing of Nashville urban emissions on July 3 and July 18, 1995, *J. Geophys. Res.*, **105**, 9155–9164, 2000.
- DeMore, W. B., S. P. Sander, D. M. Golden, R. F. Hampson, M. J. Kurylo, C. J. Howard, A. R. Ravishankara, C. E. Kolb, and M. J. Molina, Chemical kinetics and photochemical data for use in stratospheric modeling, *JPL 97-4*, Jet Propul. Lab., NASA, Pasadena, Calif., 1997.
- Dommen, J., A. S. H. Prevot, A. M. Hering, T. Staffelbach, G. L. Kok, and R. D. Schillawski, Photochemical production and the aging of an urban air mass, *J. Geophys. Res.*, **104**, 5493–5506, 1999.
- Environmental Protection Agency (EPA), Regional Interim Emission Inventories (1987–1991), vols. I and II, *EPA-454/R93-021a and b*, Research Triangle Park, N. C., 1993.
- Gery, M., W. G. Z. Whitten, J. P. Killus, and M. C. Dodge, A photochemical kinetics mechanism for urban and regional computer modeling, *J. Geophys. Res.*, **94**, 12,925–12,956, 1989.
- Godowitch, J. M., and J. M. Vukovich, 1994: Photochemical urban airshed modeling using diagnostic and dynamic meteorological fields, paper presented at 87th Air and Waste Management Association Meeting and Exhibition, Cincinnati, Ohio, June 19–24, 1994.
- Jaegle, L., D. J. Jacob, W. H. Brune, D. Tan, I. Faloona, A. J. Weinheimer, B. A. Ridley, T. L. Campos, and G. W. Sachse, Sources of HO_x and production of ozone in the upper troposphere over the United States, *Geophys. Res. Lett.*, **25**, 1705–1708, 1998.
- Jaegle, L., D. J. Jacob, W. H. Brune, and P. O. Wennberg, Chemistry of HO_x radicals in the upper troposphere, *Atmos. Environ.*, **35**, 469–490, 2001.
- Johnson, G. M., S. M. Quigley, and J. G. Smith, Management of photochemical smog using the AIRTRAK approach, in 10th International Conference of the Clean Air Society of Australia and New Zealand, pp. 209–214, Auckland, New Zealand, March, 1990.
- Kirchner, F., and W. R. Stockwell, The effect of peroxy radical reactions on the predicted concentrations of ozone, nitrogenous compounds and radicals, *J. Geophys. Res.*, **101**, 21,007–21,023, 1996.
- Kirchner, F., F. Jeaneret, A. Clappier, B. Kruger, H. van den Bergh, and B. Calpini, Total VOC reactivity in the planetary boundary layer, 2, A new indicator for determining the sensitivity of the ozone production to VOC and NO_x, *J. Geophys. Res.*, **106**, 3095–3110, 2001.
- Kleinman, L. I., Low and high-NO_x tropospheric photochemistry, *J. Geophys. Res.*, **99**, 16,831–16,838, 1994.
- Kleinman, L. I., P. H. Daum, J. H. Lee, Y.-N. Lee, L. J. Nunnermacker, S. R. Springston, L. Newman, J. Weinstein-Lloyd, and S. Sillman, Dependence of ozone production on NO and hydrocarbons in the troposphere, *Geophys. Res. Lett.*, **24**, 2299–2302, 1997.
- Lu, C.-H., and J. S. Chang, On the indicator-based approach to assess ozone sensitivities and emissions features, *J. Geophys. Res.*, **103**, 3453–3462, 1998.
- Lurmann, F. W., A. C. Lloyd, and R. Atkinson, A chemical mechanism for use in long-range transport/acid deposition computer modeling, *J. Geophys. Res.*, **91**, 10,905–10,936, 1986.
- Martilli, A., A. Nefel, G. Favaro, F. Kirchner, S. Sillman, and A. Clappier, Simulation of the ozone formation in the northern part of the P. Valley, *J. Geophys. Res.*, doi:10.1029/2001JD000534, in press, 2002.
- Morris, R. E., and T. C. Myers, User's guide for the urban airshed model, vol. I–V, *EPA-450/4-90-007A-E*, 1990.
- Odman, M. T., and C. L. Ingram, Multiscale Air Quality Simulation Platform (MAQSIP): Source code documentation and validation, *MCNC Tech. Rep. ENV-96TR002-v1.0*, 83 pp., MCNC, Research Triangle Park, N. C., 1996.
- Olszyna, K. J., E. M. Bailey, R. Simonaitis, and J. F. Meagher, O₃ and NO_y relationships at a rural site, *J. Geophys. Res.*, **99**, 14,557–14,563, 1994.
- Paulson, S. E., and J. J. Orlando, The reaction of ozone with alkenes: An important source of HO_x in the boundary layer, *Geophys. Res. Lett.*, **23**, 3727–3730, 1996.
- Paulson, S. E., and J. H. Seinfeld, Development and evaluation of a photooxidation mechanism for isoprene, *J. Geophys. Res.*, **97**, 20,703–20,715, 1992.
- Sillman, S., The use of NO_y, H₂O₂ and HNO₃ as indicators for O₃-NO_x-VOC sensitivity in urban locations, *J. Geophys. Res.*, **100**, 14,175–14,188, 1995.
- Sillman, S., J. A. Logan, and S. C. Wofsy, The sensitivity of ozone to nitrogen oxides and hydrocarbons in regional ozone episodes, *J. Geophys. Res.*, **95**, 1837–1851, 1990.
- Sillman, S., P. J. Samson, and J. M. Masters, Ozone formation in urban plumes transported over water: Photochemical model and case studies in the northeastern and midwestern U.S., *J. Geophys. Res.*, **98**, 12,687–12,699, 1993.
- Sillman, S., D. He, C. Cardelino, and R. E. Imhoff, The use of photochemical indicators to evaluate ozone-NO_x-hydrocarbon sensitivity: Case studies from Atlanta, New York and Los Angeles, *J. Air Waste Manage. Assoc.*, **47**, 642–652, September, 1997.
- Sillman, S., D. He, M. R. Pippin, P. H. Daum, D. G. Imre, L. I. Kleinman, J. H. Lee, and J. Weinstein-Lloyd, Model correlations for ozone, reactive nitrogen and peroxides for Nashville in comparison with measurements: Implications for VOC-NO_x sensitivity, *J. Geophys. Res.*, **103**, 22,629–22,644, 1998.
- Sillman, S., M. T. Odman, and A. G. Russell, Comment on “On the indicator-based approach to assess ozone sensitivities and emissions features” by C.-H. Lu and J. S. Chang, *J. Geophys. Res.*, **106**(D18), 20,941–20,944, 2001.
- Sosa, G., J. West, F. San Martini, L. T. Molina, and M. J. Molina, Air Quality Modeling and Data Analysis for Ozone and Particulates in Mexico City, *Rep. No. 15*, 76 pp., MIT Integrated Program on Urban, Reg. and Global Air Pollut., Oct. 2000.
- Stockwell, W. R., F. Kirchner, and M. Kuhn, A new mechanism for regional atmospheric chemistry modeling, *J. Geophys. Res.*, **102**, 25,847–25,879, 1997.
- Tonnesen, G. S., and R. L. Dennis, Analysis of radical propagation efficiency to assess ozone sensitivity to hydrocarbons and NO_x, 1, Local indicators of instantaneous odd oxygen production sensitivity, *J. Geophys. Res.*, **92**(13–9226), 2000a.
- Tonnesen, G. S., and R. L. Dennis, Analysis of radical propagation efficiency to assess ozone sensitivity to hydrocarbons and NO_x, 2, Long-lived species as indicators of ozone concentration sensitivity, *J. Geophys. Res.*, **92**(27–9242), 2000b.
- Trainer, M., et al., Correlation of ozone with NO_y in photochemically aged air, *J. Geophys. Res.*, **98**, 2917–2926, 1993.
- Weinstein-Lloyd, J. B., J. H. Lee, P. H. Daum, L. I. Kleinman, L. J. Nunnermacker, S. R. Springston, and L. Newman, Measurements of peroxides and related species during the 1995 summer intensive of the Southern Oxidants Study in Nashville, Tennessee, *J. Geophys. Res.*, **103**, 22,361–22,373, 1998.

D. He and S. Sillman, Department of Atmospheric, Oceanic and Space Sciences, University of Michigan, Ann Arbor, MI 48109-2143, USA.